Bond coat surface rumpling in thermal barrier coatings

Rahul Panat, Sulin Zhang, K. Jimmy Hsia*

Department of Theoretical and Applied Mechanics
University of Illinois, Urbana, IL 61801, USA

Abstract

Long term durability of thermal barrier coatings is determined by the mechanisms responsible for the nucleation and growth of interfacial cracks between coating and substrate. One such mechanism is the progressive roughening or "rumpling" of the bond coat surface upon thermal cycling. A thermodynamic analysis is presented in this paper based on a stress-driven surface diffusion mechanism to explain the bond coat rumpling process. The surface chemical potential variation required for such a diffusion process is caused by the changes in the surface energy and the elastic strain energy in the system. It is found that the amplitude of surface fluctuations with a wavelength higher than a threshold value monotonically increases with thermal cycling, while the amplitude for fluctuations with lower wavelength than the threshold value monotonically decreases. A range of wavelengths is identified to have a high monotonic amplitude increase accounting for the surface rumpling of the bond coat upon thermal cycling. This range of wavelengths obtained from the model agrees reasonably well with experimental observations.

*Corresponding author. Email: kj-hsia@uiuc.edu, Fax: 1(217) 244 5707.

Keywords: Stress driven surface diffusion; Thermally activated processes; Coating; Thin films

1 INTRODUCTION

Thermal barrier coatings (TBCs) are presently being used as protective heat resistant coatings on superalloy components in the hot sections of gas turbines [1–6]. The TBCs have been shown to reduce the operating temperature of the superalloys by as much as 180°C, improving the creep and oxidation life of the corresponding gas turbine components. A survey in early 1990s estimated that the efficiency gains resulting from the incorporation of the TBC technology could potentially save up to 40 million gallons of fuel (approximately $1 billion) a year for a fleet of 1000 aircrafts [2]. In spite of these advantages, the TBC technology has been incorporated in the gas turbine industry rather slowly.

A TBC system (Fig. 1) consists of a ceramic topcoat and an intermediate (metallic) bond coat (BC) deposited on a substrate superalloy at high temperatures. Two common deposition processes are plasma spray and electron beam physical vapor deposition (EB-PVD). The bond coat is made of either Platinum-aluminide or NiCoCrAlY alloys, while the ceramic layer is almost always made of 8% yittria-stabilized zirconia. A reaction product, thermally grown oxide (TGO), developes and grows at the BC-ceramic interface at high temperatures. The thermal expansion coefficients of these constituents of a TBC system are different, giving rise to residual stresses as the structure cools from the processing temperature.

One of the important problems limiting the use of TBCs is the long-term durability of these coatings. It has been observed that after a certain amount of service life, the coatings delaminate, exposing the underlying superalloy material. Since the local temperature in the hot section of the gas turbine can exceed the melting temperature of the superalloy, the delamination of TBCs can be very dangerous. The reasons

behind this sudden delamination are poorly understood.

While it is generally known that the final TBC failure occurs by buckling and spalling of the ceramic layer, the origin of the required critical flaw is widely debated. Some analyses in the past have pointed to the role of the TGO formed at the BC-ceramic interface in inducing the fatal flaws [7, 8]. Another mechanism, "surface rumpling" of the BC, may also induce failure flaws [9–13]. Pennefather and Boone [9] showed that platinum aluminide and NiCoCrAlY coatings of different compositions deposited on a superalloy substrate have a tendency to "rumple", i.e., to become wavy on thermal cycling. The thermal cycle employed in their experiment consisted of heating the BC-substrate to about 1050 °C in 20-25 minutes, holding the specimens at that temperature for about 45 minutes, and cooling to room temperature in about 5 minutes. The BC surfaces developed waviness with characteristic wavelengths ranging from 130-345 μm. Deb et al. [10] also found that the platinum modified as well as unmodified aluminide BC specimens showed rumpling behavior with a wavelength of about 100 μm upon thermal cycling. The thermal cycles in their experiments consisted of a 60 minute exposure at 1100°C followed by a 10 minute air cooling prior to reheating. In a recent paper, Tolpygo and Clarke [11] reported similar rumpling on platinum-modified nickel aluminide coatings. Each thermal cycle in their experiment consisted of heating and cooling of a superalloy substrate coated with platinum-modified nickel aluminide BC from room temperature to 1200°C. The heating and cooling times were about 20 minutes with a hold time of 1 hour at 1200°C. After about 100 such cycles, the surface rumpled with a wavelength of 30-50 μm and an amplitude of about 10-15 μm. On the other hand, the authors observed that when the same system was subjected to isothermal oxidation (100 hours at 1000°C), no surface rumpling occured. Fast heating and cooling rates (1050°C to 300°C temperature change in about a minute) applied to BC-superalloy system along with mechanical loading of the superalloy was also found to result in BC rumpling [12, 13] coupled with other thermal shock effects such as TGO formation and subsequent spalling or

"scalloping" [12]. In presence of the ceramic coating, the roughening caused by cyclic oxidation can give rise to cracks at the BC-ceramic interface. These cracks can then coalesce to form a crack sufficiently large to initiate delamination failure.

The present work is inspired by these observations and attempts to explain the observed surface roughening behavior in the BC materials upon thermal cycling. Here, we employ the method used to study surface roughening in semiconductor thin films [14]. These films, while being processed at 600-700°C, develop a characteristic roughness having a wavelength of hundreds of nanometers on their free surfaces. This phenomenon was explained successfully by Freund and coworkers [15–18] by assuming that the observed surface morphology is a result of stress driven surface diffusion [19–23] of the thin film material along the free surface. In the present work, a similar approach is taken to study the phenomenon of BC surface rumpling.

2 GOVERNING EQUATIONS

Similar to the studies on thin films [15–18], we consider the stress driven surface diffusion as the dominant mechanism during the BC surface morphology evolution. Further, the driving force for this diffusion is the thermal mismatch stress in the coating. The diffusion at the BC-substrate interface is neglected since it is seen to maintain its shape during roughening of the free surface of the coating [9–13]. The thermodynamic quantity that drives the shape change of the BC surface is the chemical potential. The chemical potential, under certain conditions, changes only as a result of the change in the surface energy and the elastic strain energy of the system. We can define the chemical potential, χ, on the free surface of the coating, as [15, 17],

$$\chi = (U - \kappa U_s)\Omega \tag{1}$$

where κ is the BC surface curvature, Ω is the BC atomic volume, U is the elastic strain energy per unit volume at the BC surface, and U_s is the BC surface energy

per unit area. Here U_s is taken to be a constant, γ. The variation in the chemical potential on the free surface of the coating drives the diffusion of the surface atoms. The number of atoms passing a point on the surface per unit time per unit thickness, J, is proportional to the chemical potential gradiant along the surface, and is given by the Nernst-Einstein relation [24] as,

$$J = -\frac{D_s C_s}{kT}\frac{\partial \chi}{\partial s} \tag{2}$$

where D_s is the surface diffusivity, C_s is the number of atoms per unit area, k is the Boltzman's constant, and T is the absolute temperature. Note that D_s is a function of temperature [24] given by,

$$D_s = D_0 \exp(-q/kT) \tag{3}$$

where q is the activation energy. Conservation of mass at each point along the surface of the coating results in a velocity component of the local atoms normal to the surface, V_n, (Fig. 2) given by,

$$V_n = -\Omega\frac{\partial J}{\partial s} = \frac{D_s C_s \Omega^2}{kT}\frac{\partial^2}{\partial s^2}[U - \kappa\gamma] \tag{4}$$

We now apply Eq.(4) to the problem of roughening of the coating on the superalloy. As stated before, the diffusion along the coating-substrate interface is assumed to be negligible as compared to the free surface diffusion. Thus, the coating can be modeled as a semi-infinite domain in the y direction, with thermal mismatch stress σ_T acting within the plane (Fig. 3). Note that σ_T changes with temperature, hence is a function of time in the present case of thermal cycling. This variation is given by,

$$\sigma_T = \alpha_m (T_p - T) \tag{5}$$

where α_m is a constant proportional to the themal expansion mismatch between the BC and the substrate superalloy, and T_p is the coating processing temperature. The initial bond coat surface profile is not perfectly flat. This profile can be represented

by a series of sinusoidal components such that,

$$y = h(x,t) = \sum_n a_n(t) \cos\left(\frac{2\pi x}{\lambda_n}\right) \tag{6}$$

where λ_n is the wavelength of the n-th sinusoidal component and $a_n(t)$ is the time dependent amplitude corresponding to λ_n. It is assumed that the magnitude of each $a_n(t)$ is infinitesimal, hence,

$$\frac{\partial}{\partial s} \approx \frac{\partial}{\partial x}, \quad \frac{\mathrm{d}h(x)}{\mathrm{d}x} << 1 \text{ and } \kappa = \frac{\partial^2 h}{\partial x^2} \tag{7}$$

Substituting Eqs.(6) and (7) into Eq.(4), we get,

$$\frac{\partial h}{\partial t}(x,t) = \frac{D_s C_s \Omega^2}{kT} \frac{\partial^2}{\partial x^2} \left[U(x,t) - \gamma \frac{\partial^2 h}{\partial x^2}(x,t) \right] \tag{8}$$

To determine $U(x,t)$ on the coating surface, we need to find the variation of the stress σ_T on the surface due to the slight sinusoidal fluctuations of the surface. This is derived by Gao [25], as,

$$U(x,t) = \frac{(1-\nu)\sigma_T^2}{4G} \left[1 - 8\pi \sum_n \frac{a_n(t)}{\lambda_n} \cos\left(\frac{2\pi x}{\lambda_n}\right) \right] \tag{9}$$

where ν and G are the Poisson's ratio and the shear modulus of the coating material, respectively. Substituting Eqs.(3), (6) and (9) into Eq.(8), and noting the linear independence of each sinusoidal component in Eq.(6), we obtain an ordinary differential equation governing the rumpling process of the bond coat surface,

$$\frac{\mathrm{d}a_n(t)}{\mathrm{d}t} = \frac{\beta}{T\lambda_n^3} \exp\left(-q/kT\right) \left[\frac{(1-\nu)\sigma_T^2}{G} - \left(\frac{2\pi}{\lambda_n}\right) \gamma \right] a_n(t) \tag{10}$$

where

$$\beta = \frac{8\pi^3 D_0 C_s \Omega^2}{k} \tag{10a}$$

3 CASE STUDY

We consider particular cases of thermal cycling history applied to the BC-substrate system, and solve Eq.(10) to get the time evolution of the amplitude for a given

wavelength. In gas turbines, the thermal history subjected to the TBC systems can vary widely according to the mode of application of the turbine. Systems used for propulsion and power peaking undergo multiple thermal cycles, while those used for power generation are subjected to very low frequency cycling [8]. Most of the BC rumpling experimental observations [9–13] are done with specimens subjected to multiple thermal cycles with linear heating and cooling times of the same order as the intermediate dwell times. In the present work, we consider two basic modes of thermal cycling history, triangular and sinusoidal. Rumpling behaviors for other complicated thermal histories can be deduced from these results.

3.1 Triangular temperature history

We consider the BC-substrate system experiencing triangular thermal cycles as shown in Fig.(4). The variation of the temperature in the film with time for the i-th cycle is,

$$T = \begin{cases} T_{min} + 2\,(T_{max} - T_{min})(\tau - i + 1) & i - 1 < \tau \leq i - 1/2 \\ T_{min} + 2\,(T_{max} - T_{min})(i - \tau) & i - 1/2 < \tau \leq i \end{cases} \tag{11}$$

where T_{min} and T_{max} are the minimum and the maximum temperatures, respectively, and $\tau = t/t_c$, where t_c is the time per cycle.

Due to periodicity of the problem, we can analyze the evolution of the surface fluctuation amplitude for one cycle without loss of generality. It will be seen that surface evolution for further cycles can be deduced from the same result. To obtain a solution of Eq.(10), we take $T_{min} = 300K$, $T_{max} = 1273K$, and the processing temperature $T_p = 1500K$. The BC properties are assumed to be, $\nu = 1/3$, $\gamma = 1$ J/m^2, $G = 100$ GPa and $q/(kT_p) = 2/3$. Furthermore, at $T = T_{min}$, σ_T reaches a reference stress $\sigma_\circ$ taken to be 100 MPa. Thus, from Eq.(5), $\alpha_m \approx 0.083$ MPa/K. Solving Eq.(10) using numerical integration with these values, one has,

$$\ln\left(\frac{a_n^{i+1}}{a_n^i}\right) = \frac{t_c\,\beta\,\sigma_\circ^6}{T_p\,\gamma^3\,G^3}\;\hat{\lambda_n}^{-3}\left(M - \frac{N}{\hat{\lambda_n}}\right) \tag{12}$$

where a_n^i is the amplitude of the wave with wavelength λ_n after i-th thermal cycle, $\hat{\lambda_n} = \lambda_n \sigma_o^2/(\gamma G)$ is the dimensionless wavelength, and M and N are numerical numbers independent of λ_n and t_c, determined only by the shape of the temperature history and BC properties. For the present case, $M = 1.918\times10^4$ and $N = 3.074\times10^5$. Thus, the amplitude for given thermal cycle and BC properties will change as a function of cycle time, wavelength, diffusivity, surface concentration of atomic sites, and the atomic volume. An interesting result from Eq.(12) is that the ratio of the amplitude at the end of a thermal cycle to that at the beginning is independent of the prior temperature history, and depends only on the total duration (t_c) and the shape of temperature variation of the current thermal cycle.

The amplitude ratio is plotted in Fig. 5 as a function of the wavelength, λ_n. The plot shows a wide variation in the rumpling behavior for initial fluctuations of different wavelength. For components with wavelengths less than a critical value, $\lambda_{cr}=N\gamma G/M\sigma_o^2$, the amplitude is reduced with each cycle. This value is about 156 μm in the present case. It can be seen that in this region ($\lambda_n < \lambda_{cr}$), the ratio of amplitude over each cycle decreases rapidly as the wavelength of waviness decreases. On the other hand, all components with wavelength greater than λ_{cr} increase in amplitude at varying relative rates per thermal cycle.

The result also shows that the maximum amplitude change occurs at a wavelength, $\lambda_{max}=4N\gamma G/3M\sigma_o^2$, of about 200 μm. The components with wavelengths close to this peak point undergo rapid amplitude growth. The growth of these wavelengths accounts for the observed rumpling of the BC surface as the number of cycles increases. These wavelength values are of the same order of magnitude as that observed in experiments [9–13]. The rate of amplitude increase falls rapidly beyond λ_{max} and becomes negligible for components with larger wavelengths.

Fig. 6 shows the amplitude variation with the number of thermal cycles for components with different wavelengths. The initial amplitude for all the components is taken to be unity. It can again be seen from the plot that the wave amplitude below

λ_{cr} die down fast while those above increase with varying relative rates.

3.2 Sinusoidal temperature history

We now consider a case of sinusoidal temperature history shown in Fig. 7. The temperature variation for the i-th thermal cycle is given by,

$$T = T_{min} - (T_{max} - T_{min}) \sin[\pi(\tau - i)] \qquad i - 1 < \tau \leq i \tag{13}$$

Again, due to periodicity of the problem, one thermal cycle is analyzed for the evolution of $a(t)$. The surface evolution for further cycles can be deduced from the same result. For identical BC properties and the temperature range as before, the solution to Eq.(10) has the same form as Eq.(12) with $M = 1.346 \times 10^4$ and $N = 3.137 \times 10^5$. A plot of amplitude change as a function of wavelength in Fig. 8 shows the same trend as that for the triangular temperature history. The λ_{cr} and the λ_{max} for this case are 230 μm and 310 μm, respectively.

4 DISCUSSION

The results presented here demonstrate that the analysis of BC surface rumpling based on stress driven surface diffusion provides a plausible explanation of the experimental observations reported in literature [9–13]. According to the analysis, the initial surface waviness components with wavelength close to λ_{max} (about 150- 400 μm) grow in amplitude at high relative rates upon thermal cycling. These wavelength components will eventually dominate the surface features as the number of thermal cycles increases and account for the observed nearly periodic rumpling behavior. This thermodynamic model also reveals a competition between the surface energy and the elastic strain energy in the system. The critical value of the wavelength, λ_{cr}, corresponds to a balance between these two energies. For the surface disturbances with wavelengths other than λ_{cr}, a change in the wave amplitude is energetically favored.

For example, in the case of wavelengths lower than λ_{cr}, the wave amplitude monotonically decreases with thermal cycles.

Though the present analysis is for the BC-substrate system without the ceramic topcoat, it has strong implications in the TBC failure phenomenon. In presence of the TBC layer, a restraining force will act on the BC top surface. As the BC rumples, the interface between the BC and the top ceramic coating will have a tendency to separate, causing cracking. This crack initiation process has been observed in TBC failure [8]. Once initiated, further rumpling will cause the crack to grow and eventually coalesce with adjacent ones. This is a likely mechanism by which cracks large enough to cause buckling of the ceramic topcoat can be formed on thermal cycling. Note that this model is universal for TBC failure, valid for both plasma sprayed and EB-PVD TBC systems.

The present model is applicable for tensile as well as compressive BC stresses. Mumm et al. [26] have reported that the BC is under high tensile stress at room temperature. Note that in the analysis the metallic BC layer, being thin compared to the superalloy substrate, is assumed to have negligible temperature gradient across the thickness during thermal cycling. In the case of strong temperature gradient through thickness of BC, the applicability of thermodynamics equation (1) must be re-examined.

For isothermal temperature history ($T_{max} = T_{min}$), we obtain a result similar to that by Freund et al. [15] with $\lambda_{cr} = 2\pi G\gamma/[(1-\nu)\sigma_T^2]$. The thermal expansion mismatch stress in the BC at high temperature is low, resulting in a high critical wavelength. For example, in case of $\sigma_T = 10$MPa, the critical wavelength is several millimeters. For long thermal exposures, the stresses in the TBC systems are found to relax [27–30]. This would result in a very long critical wavelength, making it impossible to observe the rumpling process. This could partly explain the lack of rumpling observed during isothermal oxidation of BC-substrate system [11, 12]. Note that the long range waviness would not have harmful effect in TBC systems. Thus, rumpling

will not be a degradation mechanism for isothermal (low frequency) exposures of the turbine blades.

The order of magnitude agreement with experiments obtained in the above analysis is quite striking, in view of the assumptions and the general uncertainty about the actual values of the parameters used. First, the BC is modeled as a homogeneous material, i. e., all the parameter values are taken to be identical everywhere. In reality, the BC has several phases across its thickness that evolve during thermal cycling. Secondly, the model does not take into account the effect of the oxide layer on the BC in the rumpling process. This oxide layer is found to locally penetrate into the BC in presence of a ceramic topcoat [26]. Previously, He et al. [31] attributed the rumpling process to ratcheting of the oxide layer on the BC, while Tolpygo and Clarke [11] speculated that a BC volume depletion process is responsible for rumpling. The former explanation indicates that rumplng is a generic process in metal-oxide systems, while the latter is not likely to lead to the developement of a characteristic rumpling wavelength. The present model based on surface diffusion, however, predicts this characteristic rumpling wavelength in reasonable agreement with experimental observations [9–13].

The present model has several assumptions and approximations. The model is applicable for the roughening process in one direction, while in experiments, the waviness occurs in two dimensions. It is also worthwhile to mention the uncertainty involved in estimating D_s and C_s. According to Asaro and Tiller [32], D_0 can vary by as much as a factor of 10^5 depanding on the environmental conditions. The activation energy, q, is usually a fraction of the chemical binding energy and is taken to be a fraction of an electron-Volt for surface atoms in the present case. The absolute value of the critical wavelength changes with this activation energy. For example, if q is increased by a factor of 5, the critical wavelength increases by a factor of 6 for sinusoidal temperature history. The authors are unaware of any experimental measurements of these BC parameters in literature. These approximations, however,

do not change the order of magnitude agreement of this model with the BC rumpling experiments [9–13].

The primary objective of the present contribution is to gain an insight into the stress driven surface diffusion as a possible mechanism of the BC surface rumpling in the BC-superalloy systems upon thermal cycling. The model predictions show reasonable agreement with the experimental observations [9–13]. The analysis establishes important parameters governing the rumpling process. These parameters can be tailored to reduce the rumpling process and avoid its harmful effects on crack initiation and growth in TBCs.

5 CONCLUSIONS

The present analysis establishes the stress driven surface diffusion as a plausible mechanism of the bond coat rumpling observed in thermal barrier coatings upon thermal cycling. This analysis predicts continuous evolution of the bond coat surface with thermal cycling. Upon each cycle, it is shown that the amplitude of the surface fluctuations with wavelength higher than a critical value monotonically increases, while the amplitude of fluctuations with wavelength lower than the critical value monotonically decreases. The analysis also establishes a range of wavelengths that have a relatively high monotonic amplitude increase. This range of wavelengths accounts for the surface rumpling of the bond coat upon thermal cycling and is shown to agree with experimental observations reported in literature.

Acknowledgement

The work is supported by a Critical Research Initiative program at the University of Illinois at Urbana-Champaign (UIUC). The authors would like to acknowledge helpful discussions with Prof. T.-C. Chiang at UIUC.

References

1. Strangman, T. E., *Thin Solid Films*, 1985, **127**, 93.

2. Sheffler, K. D. and Gupta, D. K., *J. Eng. Gas Turbine Power*, 1988, **110**, 605.

3. Meier, S. M. and Gupta, D. K., *J. Eng. Gas Turbine Power*, 1994, **116**, 250.

4. Goward, G. W., *Surf. Coat. Technol.*, 1998, **108-109**, 73.

5. Beele, W., *cfi/Ber.DKG 77*, 2000, **No. 10**, E10.

6. Stiger, M. J., Yanar, N. M., Topping, M. G., Pettit, F. S. and Meier, G. H., *Z. Metallkd.*, 1999, **90**(12), 1069.

7. Wright, P. K. and Evans, A. G., *Current Opinion in Solid State and Materials Science*, 1999, **4**, 255.

8. Evans, A. G., Mumm, D. R., Hutchinson, J. W., Meier, G. H. and Pettit, F. S., *Progress in Materials Science*, 2001, **46**, 505.

9. Pennefather, R. C. and Boone, D. H., *Surf. Coat. Technol.*, 1995, **76-77**, 47.

10. Deb, P., Boone, D. H. and Manley, T. F., II, *J. Vac. Sci. Technol.*, 1987, **5(6)**, 3366.

11. Tolpygo, V. K. and Clarke, D. R., *Acta Mater.*, 2000, **48**, 3283.

12. Holmes, J. W. and McClintock, F. A., *Metall. Trans.*, 1990, **21A**, 1209.

13. Zhang, Y. H., Withers, P. J., Fox, M. D. and Knowles, D. M., *Materials Science and Technology*, 1999, **15**, 1031.

14. Gao, H. and Nix, W. D., *Annu. Rev. Mater. Sci.*, 1999, **29**, 173.

15. Freund, L. B., Beltz, G. E. and Jonsdottir, F., *Mat. Res. Symp. Proc.*, 1993, **3**(8), 383.

16. Freund, L. B. and Jonsdottir, F., *J. Mech. Phys. Solids*, 1993, **41**, 1245.

17. Freund, L. B., *Int. J. Solids Structures*, 1995, **32**(6/7), 911.

18. Freund, L. B. and Jonsdottir, F., *Mechanics of Materials*, 1995, **20**, 337.

19. Grilhe, J., *Acta Metall. Mater.*, 1993, **41**, 909.

20. Grinfeld, M. A., *J. Nonlinear Sci.*, 1993, **3**, 35.

21. Srolovitz D. J., *Acta Metall.*, 1989, **37**(2), 621.

22. Gao, H., *J. Mech. Phys. Solids*, 1994, **42**(5), 741.

23. Suo, Z., *J. Mech. Phys. Solids*, 1995, **43**(6), 829.

24. Shewmon, P. G., *Diffusion in solids*, 2nd edition, Minerals, Metals & Materials Society, 1989, pp. 30.

25. Gao, H., *J. Mech. Phys. Solids*, 1991, **39**, 443.

26. Mumm, D. R., Evans, A. G. and Spitsberg, I. T., *Acta Mater.*, 2001, **49**, 2339.

27. Strangman, T. E. and Hopkins, S. W., *Am. Ceram. Soc. Bull.*, 1971, **55**, 304.

28. McDonald, G. and Hendricks, R. C., *Thin Solid Films*, 1980, **73**, 491.

29. Miller, R. A. and Lowell, C. E., *Thin Solid Films*, 1982, **95**, 265.

30. Jordan, D. W. and Faber, K. T., *Thin Solid Films*, 1993, **235**, 137.

31. He, M. Y., Evans, A. G. and Hutchinson, J. W., *Acta Mater.*, 2000, **48**, 2593.

32. Asaro, R. J. and Tiller, W. A., *Metall. Trans.*, 1972, **42**, 1789.

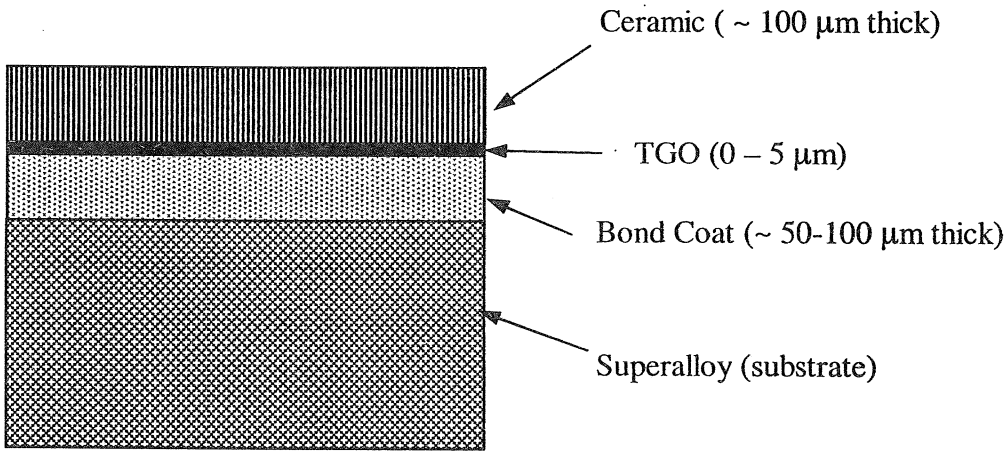

Figure 1: TBC structure

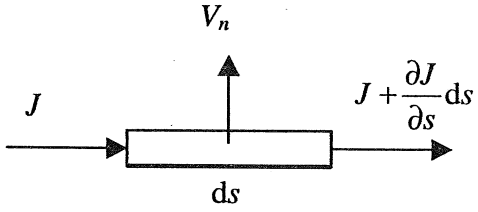

Figure 2: Diffusion along surface element of the coating

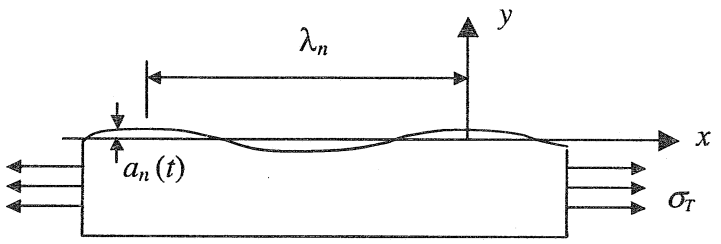

Figure 3: Sinusoidal fluctuations of the free surface of BC

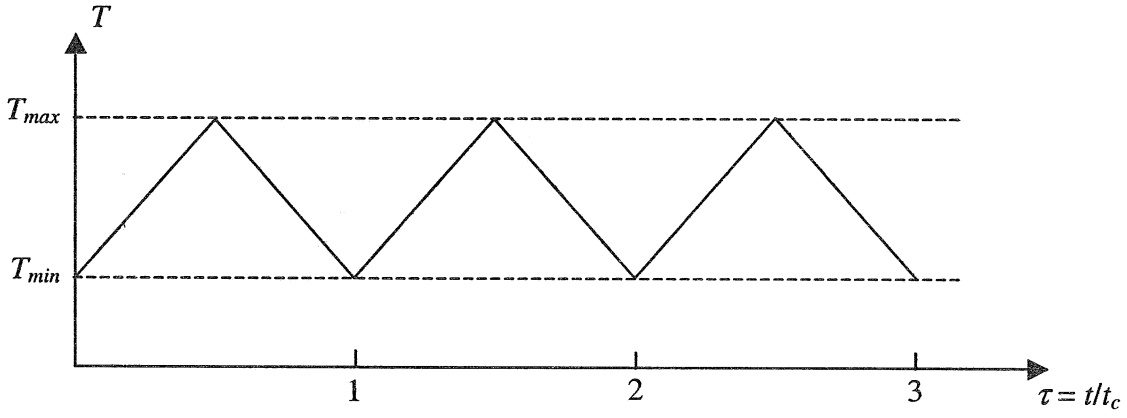

Figure 4: Thermal cycling with triangular temperature variation with normalized time

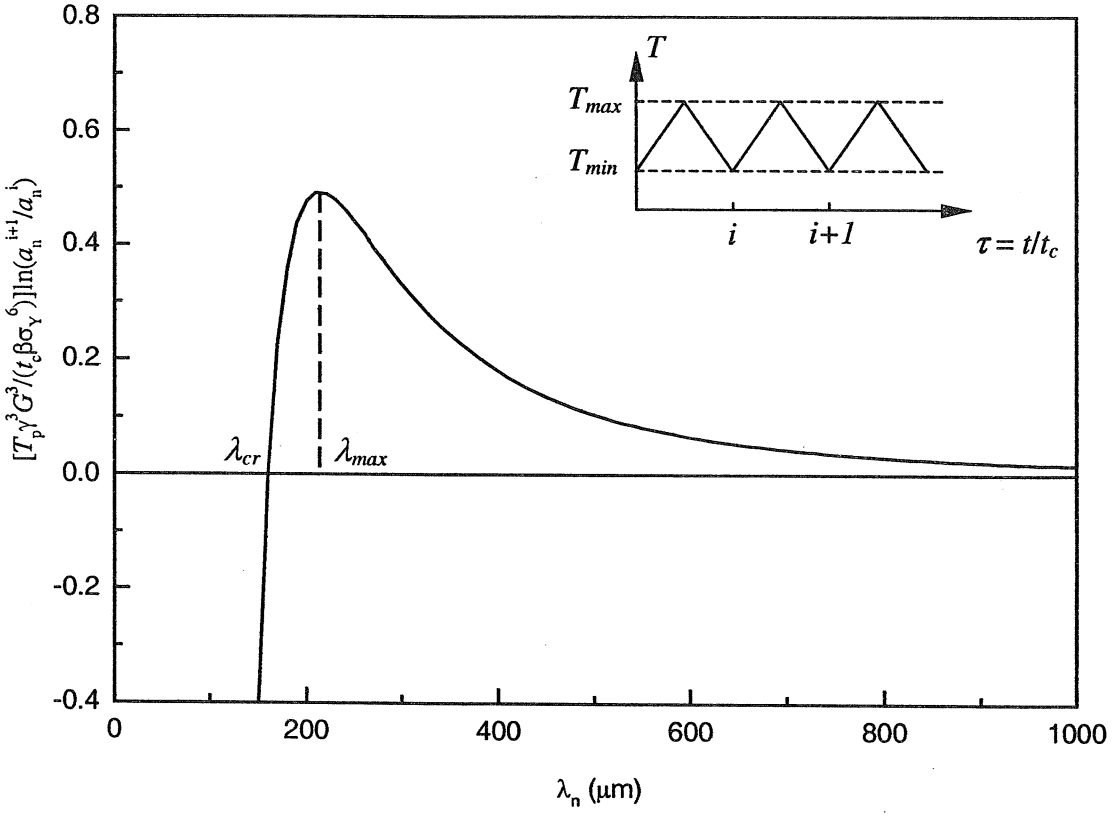

Figure 5: Ratio of amplitude change after one thermal cycle as a function of wavelength

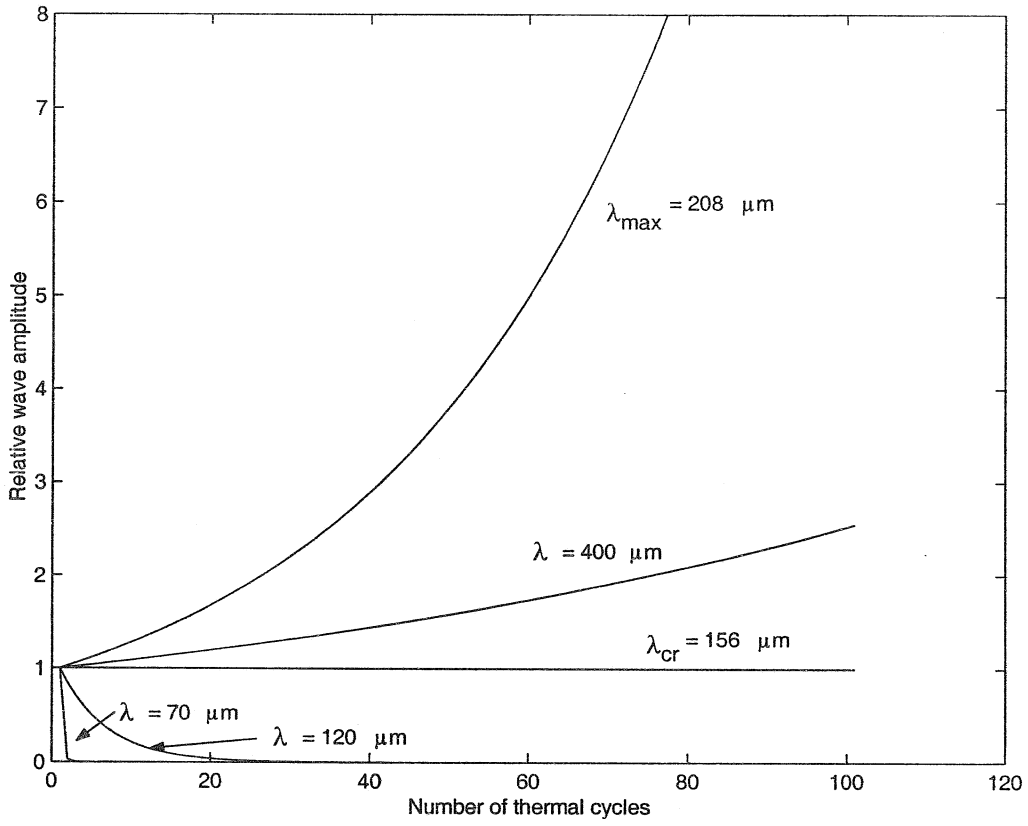

Figure 6: Relative wave amplitude as a function of the number of thermal cycles for different wavelengths

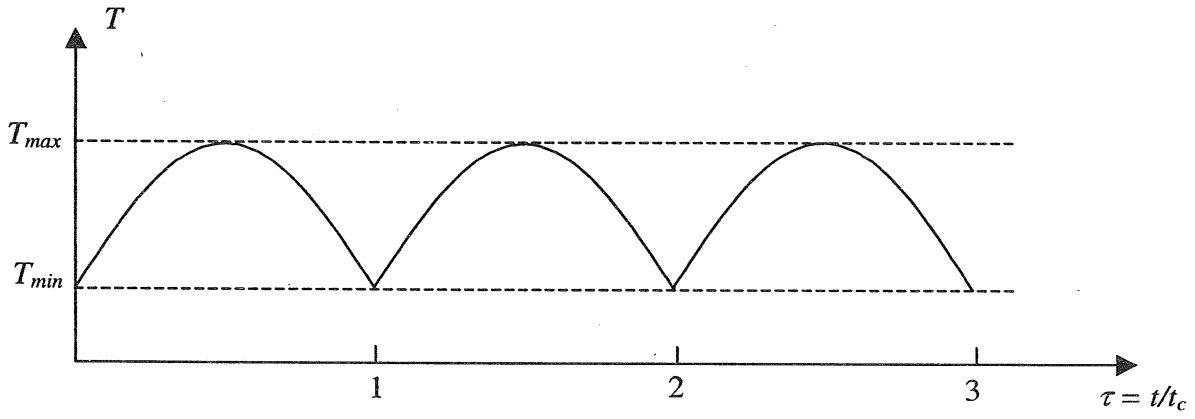

Figure 7: Thermal cycling with sinusoidal temperature variation with normalized time

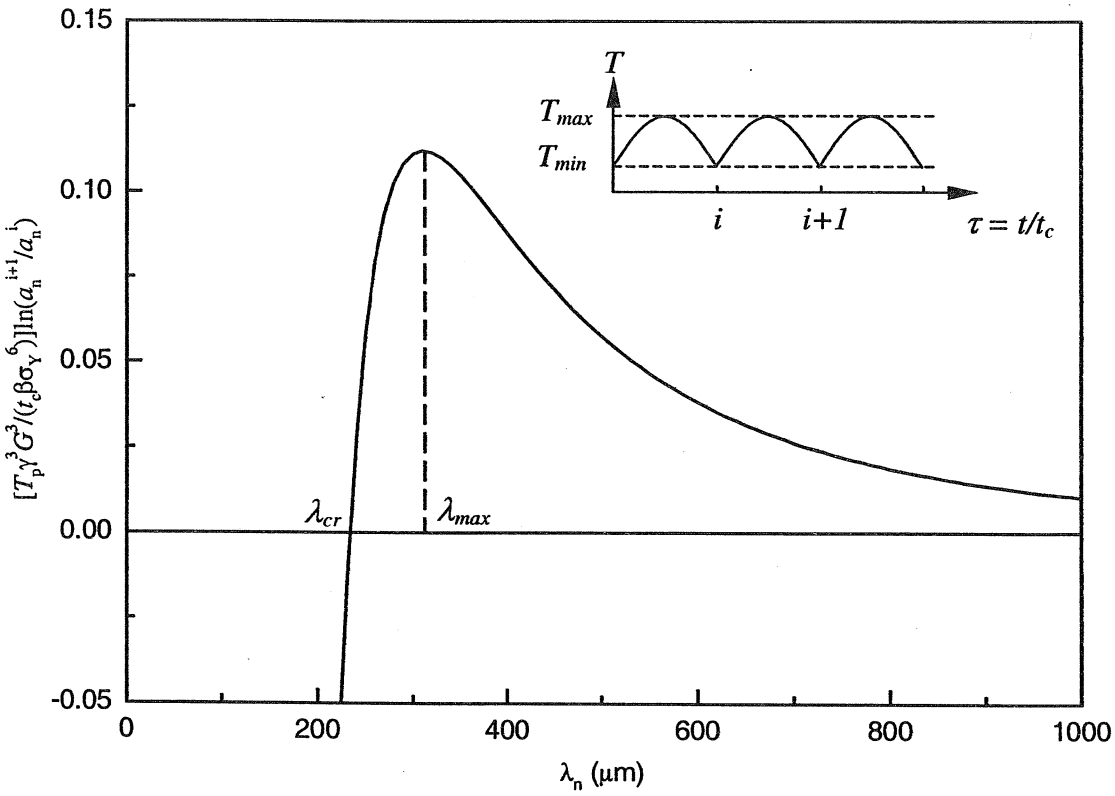

Figure 8: Ratio of amplitude change after one thermal cycle as a function of wavelength

List of Recent TAM Reports

No.	Authors	Title	Date
908	Aref, H., and M. A. Stremler	Four-vortex motion with zero total circulation and impulse—*Physics of Fluids* **11,** 3704-3715	May 1999
909	Adrian, R. J., K. T. Christensen, and Z.-C. Liu	On the analysis and interpretation of turbulent velocity fields—*Experiments in Fluids* **29,** 275–290 (2000)	May 1999
910	Fried, E., and S. Sellers	Theory for atomic diffusion on fixed and deformable crystal lattices—*Journal of Elasticity* **59,** 67–81 (2000)	June 1999
911	Sofronis, P., and N. Aravas	Hydrogen induced shear localization of the plastic flow in metals and alloys—*European Journal of Mechanics/A Solids* (submitted)	June 1999
912	Anderson, D. R., D. E. Carlson, and E. Fried	A continuum-mechanical theory for nematic elastomers—*Journal of Elasticity* **56,** 33–58 (1999)	June 1999
913	Riahi, D. N.	High Rayleigh number convection in a rotating melt during alloy solidification—*Recent Developments in Crystal Growth Research* **2,** 211–222 (2000)	July 1999
914	Riahi, D. N.	Buoyancy driven flow in a rotating low Prandtl number melt during alloy solidification—*Current Topics in Crystal Growth Research* **5,** 151–161 (2000)	July 1999
915	Adrian, R. J.	On the physical space equation for large-eddy simulation of inhomogeneous turbulence—*Physics of Fluids* (submitted)	July 1999
916	Riahi, D. N.	Wave and vortex generation and interaction in turbulent channel flow between wavy boundaries—*Journal of Mathematical Fluid Mechanics* (submitted)	July 1999
917	Boyland, P. L., M. A. Stremler, and H. Aref	Topological fluid mechanics of point vortex motions	July 1999
918	Riahi, D. N.	Effects of a vertical magnetic field on chimney convection in a mushy layer—*Journal of Crystal Growth* **216,** 501–511 (2000)	Aug. 1999
919	Riahi, D. N.	Boundary mode–vortex interaction in turbulent channel flow over a non-wavy rough wall—*Proceedings of the Royal Society of London A,* **457,** 2643–2666 (2001)	Sept. 1999
920	Block, G. I., J. G. Harris, and T. Hayat	Measurement models for ultrasonic nondestructive evaluation—*IEEE Transactions on Ultrasonics, Ferroelectrics, and Frequency Control* **47,** 604–611 (2000)	Sept. 1999
921	Zhang, S., and K. J. Hsia	Modeling the fracture of a sandwich structure due to cavitation in a ductile adhesive layer—*Journal of Applied Mechanics* **68,** 93–100 (2001)	Sept. 1999
922	Nimmagadda, P. B. R., and P. Sofronis	Leading order asymptotics at sharp fiber corners in creeping-matrix composite materials	Oct. 1999
923	Yoo, S., and D. N. Riahi	Effects of a moving wavy boundary on channel flow instabilities—*Theoretical and Computational Fluid Dynamics* (submitted)	Nov. 1999
924	Adrian, R. J., C. D. Meinhart, and C. D. Tomkins	Vortex organization in the outer region of the turbulent boundary layer—*Journal of Fluid Mechanics* **422,** 1–53 (2000)	Nov. 1999
925	Riahi, D. N., and A. T. Hsui	Finite amplitude thermal convection with variable gravity—*International Journal of Mathematics and Mathematical Sciences* **25,** 153–165 (2001)	Dec. 1999
926	Kwok, W. Y., R. D. Moser, and J. Jiménez	A critical evaluation of the resolution properties of *B*-spline and compact finite difference methods—*Journal of Computational Physics* (submitted)	Feb. 2000
927	Ferry, J. P., and S. Balachandar	A fast Eulerian method for two-phase flow—*International Journal of Multiphase Flow,* in press (2000)	Feb. 2000
928	Thoroddsen, S. T., and K. Takehara	The coalescence–cascade of a drop—*Physics of Fluids* **12,** 1257–1265 (2000)	Feb. 2000
929	Liu, Z.-C., R. J. Adrian, and T. J. Hanratty	Large-scale modes of turbulent channel flow: Transport and structure—*Journal of Fluid Mechanics* (submitted)	Feb. 2000

List of Recent TAM Reports (cont'd)

No.	Authors	Title	Date
930	Borodai, S. G., and R. D. Moser	The numerical decomposition of turbulent fluctuations in a compressible boundary layer—*Theoretical and Computational Fluid Dynamics* (submitted)	Mar. 2000
931	Balachandar, S., and F. M. Najjar	Optimal two-dimensional models for wake flows—*Physics of Fluids*, in press (2000)	Mar. 2000
932	Yoon, H. S., K. V. Sharp, D. F. Hill, R. J. Adrian, S. Balachandar, M. Y. Ha, and K. Kar	Integrated experimental and computational approach to simulation of flow in a stirred tank—*Chemical Engineering Sciences* (submitted)	Mar. 2000
933	Sakakibara, J., Hishida, K., and W. R. C. Phillips	On the vortical structure in a plane impinging jet—*Journal of Fluid Mechanics* **434**, 273–300 (2001)	Apr. 2000
934	Phillips, W. R. C.	Eulerian space–time correlations in turbulent shear flows—*Physics of Fluids* **12**, 2056–2064 (2000)	Apr. 2000
935	Hsui, A. T., and D. N. Riahi	Onset of thermal–chemical convection with crystallization within a binary fluid and its geological implications—*Geochemistry, Geophysics, Geosystems* **2**, 2000GC000075 (2001)	Apr. 2000
936	Cermelli, P., E. Fried, and S. Sellers	Configurational stress, yield, and flow in rate-independent plasticity—*Proceedings of the Royal Society of London A* **457**, 1447–1467 (2001)	Apr. 2000
937	Adrian, R. J., C. Meneveau, R. D. Moser, and J. J. Riley	Final report on 'Turbulence Measurements for Large-Eddy Simulation' workshop	Apr. 2000
938	Bagchi, P., and S. Balachandar	Linearly varying ambient flow past a sphere at finite Reynolds number—Part 1: Wake structure and forces in steady straining flow	Apr. 2000
939	Gioia, G., A. DeSimone, M. Ortiz, and A. M. Cuitiño	Folding energetics in thin-film diaphragms—*Proceedings of the Royal Society of London A*, in press (2001)	Apr. 2000
940	Chaïeb, S., and G. H. McKinley	Mixing immiscible fluids: Drainage induced cusp formation	May 2000
941	Thoroddsen, S. T., and A. Q. Shen	Granular jets—*Physics of Fluids* **13**, 4–6 (2001)	May 2000
942	Riahi, D. N.	Non-axisymmetric chimney convection in a mushy layer under a high-gravity environment—In *Centrifugal Materials Processing* (L. L. Regel and W. R. Wilcox, eds.), 295–302 (2001)	May 2000
943	Christensen, K. T., S. M. Soloff, and R. J. Adrian	PIV Sleuth: Integrated particle image velocimetry interrogation/validation software	May 2000
944	Wang, J., N. R. Sottos, and R. L. Weaver	Laser induced thin film spallation—*Experimental Mechanics* (submitted)	May 2000
945	Riahi, D. N.	Magnetohydrodynamic effects in high gravity convection during alloy solidification—In *Centrifugal Materials Processing* (L. L. Regel and W. R. Wilcox, eds.), 317–324 (2001)	June 2000
946	Gioia, G., Y. Wang, and A. M. Cuitiño	The energetics of heterogeneous deformation in open-cell solid foams—*Proceedings of the Royal Society of London A* **457**, 1079–1096 (2001)	June 2000
947	Kessler, M. R., and S. R. White	Self-activated healing of delamination damage in woven composites—*Composites A: Applied Science and Manufacturing* **32**, 683–699 (2001)	June 2000
948	Phillips, W. R. C.	On the pseudomomentum and generalized Stokes drift in a spectrum of rotational waves—*Journal of Fluid Mechanics* **430**, 209–229 (2001)	July 2000
949	Hsui, A. T., and D. N. Riahi	Does the Earth's nonuniform gravitational field affect its mantle convection?—*Physics of the Earth and Planetary Interiors* (submitted)	July 2000

List of Recent TAM Reports (cont'd)

No.	Authors	Title	Date
950	Phillips, J. W.	Abstract Book, 20th International Congress of Theoretical and Applied Mechanics (27 August – 2 September, 2000, Chicago)	July 2000
951	Vainchtein, D. L., and H. Aref	Morphological transition in compressible foam—*Physics of Fluids* **13**, 2152–2160 (2001)	July 2000
952	Chaïeb, S., E. Sato-Matsuo, and T. Tanaka	Shrinking-induced instabilities in gels	July 2000
953	Riahi, D. N., and A. T. Hsui	A theoretical investigation of high Rayleigh number convection in a nonuniform gravitational field—*Acta Mechanica* (submitted)	Aug. 2000
954	Riahi, D. N.	Effects of centrifugal and Coriolis forces on a hydromagnetic chimney convection in a mushy layer—*Journal of Crystal Growth* **226**, 393–405 (2001)	Aug. 2000
955	Fried, E.	An elementary molecular-statistical basis for the Mooney and Rivlin–Saunders theories of rubber-elasticity—*Journal of the Mechanics and Physics of Solids*, in press (2001)	Sept. 2000
956	Phillips, W. R. C.	On an instability to Langmuir circulations and the role of Prandtl and Richardson numbers—*Journal of Fluid Mechanics* **442**, 335–358 (2001)	Sept. 2000
957	Chaïeb, S., and J. Sutin	Growth of myelin figures made of water soluble surfactant—Proceedings of the 1st Annual International IEEE–EMBS Conference on Microtechnologies in Medicine and Biology (October 2000, Lyon, France), 345–348	Oct. 2000
958	Christensen, K. T., and R. J. Adrian	Statistical evidence of hairpin vortex packets in wall turbulence—*Journal of Fluid Mechanics* **431**, 433–443 (2001)	Oct. 2000
959	Kuznetsov, I. R., and D. S. Stewart	Modeling the thermal expansion boundary layer during the combustion of energetic materials—*Combustion and Flame*, in press (2001)	Oct. 2000
960	Zhang, S., K. J. Hsia, and A. J. Pearlstein	Potential flow model of cavitation-induced interfacial fracture in a confined ductile layer—*Journal of the Mechanics and Physics of Solids*, in press (2002)	Nov. 2000
961	Sharp, K. V., R. J. Adrian, J. G. Santiago, and J. I. Molho	Liquid flows in microchannels—Chapter 6 of *CRC Handbook of MEMS* (M. Gad-el-Hak, ed.) (2001)	Nov. 2000
962	Harris, J. G.	Rayleigh wave propagation in curved waveguides—*Wave Motion*, in press (2001)	Jan. 2001
963	Dong, F., A. T. Hsui, and D. N. Riahi	A stability analysis and some numerical computations for thermal convection with a variable buoyancy factor—*Geophysical and Astrophysical Fluid Dynamics* (submitted)	Jan. 2001
964	Phillips, W. R. C.	Langmuir circulations beneath growing or decaying surface waves—*Journal of Fluid Mechanics* (submitted)	Jan. 2001
965	Bdzil, J. B., D. S. Stewart, and T. L. Jackson	Program burn algorithms based on detonation shock dynamics—*Journal of Computational Physics* (submitted)	Jan. 2001
966	Bagchi, P., and S. Balachandar	Linearly varying ambient flow past a sphere at finite Reynolds number: Part 2—Equation of motion—*Journal of Fluid Mechanics* (submitted)	Feb. 2001
967	Cermelli, P., and E. Fried	The evolution equation for a disclination in a nematic fluid—*Proceedings of the Royal Society A*, in press (2001)	Apr. 2001
968	Riahi, D. N.	Effects of rotation on convection in a porous layer during alloy solidification—Chapter in *Transport Phenomena in Porous Media* (D. B. Ingham and I. Pop, eds.), Oxford: Elsevier Science (2001)	Apr. 2001
969	Damljanovic, V., and R. L. Weaver	Elastic waves in cylindrical waveguides of arbitrary cross section—*Journal of Sound and Vibration* (submitted)	May 2001
970	Gioia, G., and A. M. Cuitiño	Two-phase densification of cohesive granular aggregates	May 2001

List of Recent TAM Reports (cont'd)

No.	Authors	Title	Date
971	Subramanian, S. J., and P. Sofronis	Calculation of a constitutive potential for isostatic powder compaction—*International Journal of Mechanical Sciences* (submitted)	June 2001
972	Sofronis, P., and I. M. Robertson	Atomistic scale experimental observations and micromechanical/continuum models for the effect of hydrogen on the mechanical behavior of metals—*Philosophical Magazine* (submitted)	June 2001
973	Pushkin, D. O., and H. Aref	Self-similarity theory of stationary coagulation—*Physics of Fluids* (submitted)	July 2001
974	Lian, L., and N. R. Sottos	Stress effects in ferroelectric thin films—*Journal of the Mechanics and Physics of Solids* (submitted)	Aug. 2001
975	Fried, E., and R. E. Todres	Prediction of disclinations in nematic elastomers—*Proceedings of the National Academy of Sciences*, in press (2002)	Aug. 2001
976	Fried, E., and V. A. Korchagin	Striping of nematic elastomers—*International Journal of Solids and Structures*, in press (2002)	Aug. 2001
977	Riahi, D. N.	On nonlinear convection in mushy layers: Part I. Oscillatory modes of convection—*Journal of Fluid Mechanics* (submitted)	Sept. 2001
978	Sofronis, P., I. M. Robertson, Y. Liang, D. F. Teter, and N. Aravas	Recent advances in the study of hydrogen embrittlement at the University of Illinois—Invited paper, Hydrogen–Corrosion Deformation Interactions (Sept. 16–21, 2001, Jackson Lake Lodge, Wyo.)	Sept. 2001
979	Fried, E., M. E. Gurtin, and K. Hutter	A void-based description of compaction and segregation in flowing granular materials—*Proceedings of the Royal Society of London A* (submitted)	Sept. 2001
980	Adrian, R. J., S. Balachandar, and Z.-C. Liu	Spanwise growth of vortex structure in wall turbulence—Korean Society of Mechanical Engineers special issue on Flow Visualization (December 2001)	Sept. 2001
981	Adrian, R. J.	Information and the study of turbulence and complex flow—*Japanese Society of Mechanical Engineers B* (submitted)	Oct. 2001
982	Adrian, R. J., and Z.-C. Liu	Observation of vortex packets in direct numerical simulation of fully turbulent channel flow—*Journal of Visualization* (submitted)	Oct. 2001
983	Fried, E., and R. E. Todres	Disclinated states in nematic elastomers—*Journal of the Mechanics and Physics of Solids* (submitted)	Oct. 2001
984	Stewart, D. S.	Towards the miniaturization of explosive technology—Proceedings of the 23rd International Conference on Shock Waves (2001)	Oct. 2001
985	Kasimov, A. R., and Stewart, D. S.	Spinning instability of gaseous detonations—*Journal of Fluid Mechanics* (submitted)	Oct. 2001
986	Brown, E. N., N. R. Sottos, and S. R. White	Fracture testing of a self-healing polymer composite—*Experimental Mechanics* (submitted)	Nov. 2001
987	Phillips, W. R. C.	Langmuir circulations—*Surface Waves* (J. C. R. Hunt and S. Sajjadi, eds.), in press (2002)	Nov. 2001
988	Gioia, G., and F. A. Bombardelli	Scaling and similarity in rough channel flows—*Physical Review Letters*, in press (2001)	Nov. 2001
989	Riahi, D. N.	On stationary and oscillatory modes of flow instabilities in a rotating porous layer during alloy solidification—*Journal of Porous Media* (submitted)	Nov. 2001
990	Okhuysen, B. S., and D. N. Riahi	Effect of Coriolis force on instabilities of liquid and mushy regions during alloy solidification—*Physics of Fluids* (submitted)	Dec. 2001
991	Christensen, K. T., and R. J. Adrian	Measurement of instantaneous Eulerian acceleration fields by particle-image accelerometry: Method and accuracy—*Experimental Fluids* (submitted)	Dec. 2001
992	Liu, M., and K. J. Hsia	Interfacial cracks between piezoelectric and elastic materials under in-plane electric loading—*Journal of the Mechanics and Physics of Solids* (submitted)	Dec. 2001
993	Panat, R. P., S. Zhang, and K. J. Hsia	Bond coat surface rumpling in thermal barrier coatings—*Acta Materialia* (submitted)	Jan. 2002